buildings

MDPI

Article

Investigation into the Characteristics of Expansion and Compression Deformation of Interbedded Weak Expansive Rocks in Water Immersion

Yaning Wang [1], Yuchen Li [2], Haoyu Qin [2], Yangui Zhu [1], Yibo Yao [1], Jin Jin [1], Tao Zheng [1], Qingting Qian [2] and De Chen [2,3,*]

[1] China Railway First Survey and Design Institute Group Co., Ltd., Xi'an 710043, China
[2] School of Civil Engineering, Southwest Jiaotong University, Chengdu 610031, China
[3] Key Laboratory of High-Speed Railway Engineering of Ministry of Education, Southwest Jiaotong University, Chengdu 610031, China
* Correspondence: chende@swjtu.edu.cn

Abstract: In order to investigate the deformation characteristics of interbedded weak expansive rocks in water immersion, the sandstone–mudstone interbedded structures were taken as the object of this study. A total of 27 sets of indoor immersion tests were designed with three influencing factors, namely, the layer thickness ratios of sandstone and mudstone (1:1, 2:1, 3:1), the occurrence of the rock layers (flat, oblique, and vertical), and the overburden loadings (0 kPa, 12.5 kPa, and 25 kPa). Tests were conducted to obtain the deformation time series data of the samples during the immersion loading process. Based on this, the influence pattern of each influencing factor on the sample deformation was analyzed individually. The results show that with the increase in overburden loading and rock inclination angle, the sample develops from expansion deformation to compression deformation. Changes in the layer thickness ratio will not change the deformation trend of the sample, and the decrease in the relative mudstone content will only reduce the absolute value of the sample's expansion and compression deformation. The deformation stability rate of the sample under load is 5~7 times that under no load. The increase in layer thickness ratio and rock inclination angle will lead to different degrees of attenuation of sample expansion force in the range of 8.91~38.68% and 51.00~58.83%, respectively. The research results of this paper can provide a meaningful reference for the design and maintenance of a high-speed railway subgrade in a weak expansive rock area with an interbedded structure.

Keywords: subgrade engineering; weak expansive rocks; interbedded structure; indoor water immersion test; expansion and compression deformation

Citation: Wang, Y.; Li, Y.; Qin, H.; Zhu, Y.; Yao, Y.; Jin, J.; Zheng, T.; Qian, Q.; Chen, D. Investigation into the Characteristics of Expansion and Compression Deformation of Interbedded Weak Expansive Rocks in Water Immersion. *Buildings* **2024**, *14*, 1901. https://doi.org/10.3390/buildings14071901

Academic Editor: Humberto Varum

Received: 9 April 2024
Revised: 7 June 2024
Accepted: 8 June 2024
Published: 21 June 2024

1. Introduction

Layered rock mass has obvious layered structures such as a stratification plane and a schistosity plane. As one of the special structures, interbedded rocks are characterized by the repeated alternation of two or more lithology strata due to the continuous change in the sedimentary environment, which is usually manifested as the difference in rock hardness [1]. Compared to a single homogeneous rock mass, interbedded rock mass exhibits a high degree of anisotropy [2]. Due to the change in boundary conditions such as a complex in situ stress environment, excavation, and support, and the influence of environmental factors such as rainfall, evaporation, and the freeze–thaw cycle, its deformation and failure mechanism is very complex. Geotechnical structures over the long-term serving in such complex environments face severe safety challenges. Therefore, it is necessary to explore the basic mechanical behavior and deformation failure mechanism of the interbedded rock mass. This is of great practical significance to ensure the rational design and safe service of geotechnical structures in such areas.

Scholars first focused on the study of mechanical properties and deformation mechanisms of interbedded rock mass. They are accustomed to conducting numerical simulation inversion analyses of the structural damage based on experimental data, and then introducing a structural response into the calculation model, which is compared with the field monitoring data to verify the validity of the model [3,4]. Maheshwari [5] used the elastic–viscoelastic correspondence principle to explain the long-term viscoelastic response caused by underground excavations in the layered rock mass, and proposed a simple calculation method for the deformation of the layered rock mass. Wu et al. [6] conducted different times of wet–dry cycle tests on 116 silty mudstone and silty sandstone samples. The test results reveal the strength-weakening characteristics and mechanisms of these two types of rocks. Through the established strength-weakening model, they discussed the influence of the wet–dry cycle on the strength of soft–hard interbedded rock mass. In recent years, many new techniques have been applied to the preparation and failure characterization of interbedded rock samples. Tian et al. [7] used 3D-printing sand core technology to prepare soft–hard interbedded rock mass samples with different inclination angles. The deformation difference between soft and hard rocks is verified by the captured digital images, and the anisotropic failure evolution mode of soft–hard interbedded rock mass is revealed. Luo et al. [8] explored the strain evolution and crack propagation process of soft–hard interbedded composite rock-like samples by digital image correlation (DIC) technology. A simplified mechanical model of interbedded rock mass under uniaxial compression has also been established.

The stability problem of interbedded rock slopes is very prominent. Frequent geological disasters pose a great threat to the safety of engineering and personnel [9–11]. Some scholars have obtained the engineering characteristics of the slope through on-site geological surveys. By combining indoor tests and numerical simulations, the deformation and failure mechanism of an interbedded structure slope has been explored. On this basis, the failure evolution process of the slope is divided into stages with different characteristics [12–15]. Safety evaluation is also the research focus in the field of slope engineering [16]. Wyllie and Wood [17,18] verified the feasibility of the limit equilibrium method to analyze toppling deformation by several examples of anti-dip rock slope engineering. Liu et al. [19] established an independent cantilever beam model based on the theory of fracture mechanics, and then proposed an improved calculation method for the stability of soft and hard interbedded anti-dip rock slopes. Based on the deformation compatibility of rock mass, Wang et al. [20] proposed a theoretical method for evaluating the stability of soft and hard interbedded anti-dip rock slopes, namely, DCM.

The upper and lower rock masses of the interbedded surrounding rock are uneven in hardness and poor in self-stability. The surrounding rock is easy to slide or bend along the inclined rock surface due to excavation disturbance, resulting in a bias phenomenon. Local stress concentration and excessive deformation will promote the initiation and propagation of cracks. When this is serious, it will lead to shear failure of the tunnel structure [21,22]. Previous studies have mainly focused on exploring the stress distribution characteristics and failure evolution law of tunnels in a single-lithologic layered rock mass. But a unified understanding has not yet been formed. In recent years, research results on the large deformation mechanism of soft and hard interbedded surrounding rock tunnels have been emerging. Zhao et al. [23] took the Zhengzhou–Wanzhou high-speed railway mudstone-interbedded–sandstone-bedding rock tunnel as the research object. The effects of burial depth, bedding dip angle and spacing, and groundwater on the pressure and deformation characteristics of the tunnel surrounding rock were investigated. They also revealed the failure mechanism of large-span bedding tunnel lining. Based on the field monitoring data, Liu and Chen et al. [24,25] analyzed the deformation characteristics and failure modes of the Muzhailing tunnel. They divided the evolution process of tunnel large deformation into five stages: premise, gestation, development, occurrence, and treatment.

The sandstone–mudstone interbedded structure is widely distributed all over the world, especially in the southwest, northwest, central, and southern regions of China [26]. A

large number of studies have shown that mudstone and sandstone have weak expansibility and will expand and soften in water [27]. With the continuous growth of high-speed railway construction mileage in the world, the problem of subgrade uplift deformation caused by expansive rock is becoming more and more prominent. The strict requirements of track smoothness limit the popularization and application of the ballastless track in such areas. In recent years, some scholars have made useful explorations on the above issues. Dai et al. [28] obtained the expansive characteristics of red-bed mudstone by taking the subgrade of Neijiang North Railway Station as an example. They proposed a decoupling analysis method of seepage and swelling to invert and predict the uplift deformation of the subgrade. According to the field deformation monitoring results of the subgrade, Wang et al. [4] analyzed the influence of the expansion rate of the subgrade filler and mudstone foundation on the uplift response of the ballastless track. Then, they gave the prediction method of uplift based on the numerical calculation results. Some scholars have used a physical model test, an in situ test, and other methods in practice. On this basis, they explored the mechanical behavior and deformation characteristics of the subgrade in an expansive rock area under water immersion conditions [29–35].

Although there are a considerable number of research results on interbedded rock mass, they are mainly concentrated in the fields of slope and tunnel engineering. There are relatively few studies on the deformation response of a sandstone–mudstone interbedded structure, which is often encountered in the practice of high-speed railway subgrade engineering. In addition, the existing research is mostly limited to the influence of the engineering characteristics of a single expansive rock on the deformation of the subgrade [36–39]. Few studies have been reported on weak expansive rocks, which consider the complex deformation and damage mechanisms. In addition, in order to better control the parameters such as layer thickness ratio, inclination angle, and loading, most of the existing studies used similar materials to prepare samples [40,41]. Some scholars used numerical simulation or other methods [42] to analyze the deformation characteristics of interbedded rock mass. However, the results obtained by these methods are difficult to truly reflect the deformation characteristics of weak expansive rocks with an interbedded structure in a natural state.

Based on the above problems, this study took the sandstone–mudstone interbedded structures as the research object. This research utilized a self-designed expansion and compression deformation characterization test equipment to design 27 sets of indoor immersion tests. These were based on three influencing factors: the thickness ratio of sandstone and mudstone, the occurrence of rock mass, and the overburden loading. Tests were conducted to obtain the deformation time series data of the samples during the immersion loading process. Based on this, the influence pattern of each influencing factor on the sample deformation was analyzed individually. The research results are expected to provide a valuable reference for the rational design, operation, and maintenance of a ballastless track subgrade of a high-speed railway in a weak expansive rock area with an interbedded structure.

2. Experimental Scheme Design

2.1. Test Equipment

The research team developed a specialized testing apparatus to investigate the expansion and compression deformation characteristics of weak expansive rocks with a typical sandstone intercalated with mudstone interbedded structure when immersed in water. This apparatus, depicted in Figure 1, is designed to measure the expansion and compression deformation characteristics of weak expansive rocks under applied loads. The primary components of the equipment include a sample model box, a hydraulic loading system, a force sensor, and an array of displacement sensors.

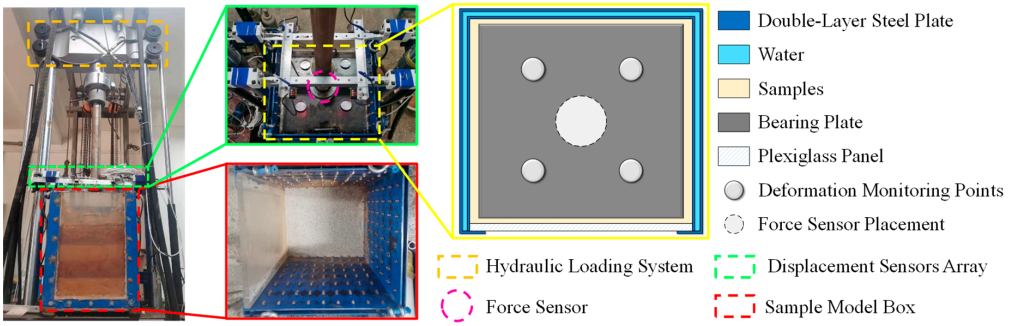

Figure 1. Expansion and compression deformation characterization test equipment.

The sample model box, constructed with reference to the dimensions of a large-scale dynamic triaxial test (300 mm × 600 mm), features an internal loading space measuring 475 mm in length, 440 mm in width, and 600 mm in height. The box is fabricated from a double-layer steel plate, welded and fitted with a high-strength transparent plexiglass panel bolted to the front side. This design allows for easy observation and documentation of the layer thickness ratio, occurrence, and deformation of sandstone and mudstone interbedded structure samples during the loading process. A 10 mm gap between the double-layer steel plates accommodates even distribution of water permeation holes on the inner steel plate's surface, promoting rapid immersion and saturation of the samples in a tri-directional water environment. Any excess water can be efficiently drained through a water valve located at the bottom rear of the sample model box.

The hydraulic loading system is an electro-hydraulic servo with a single-channel pseudo-dynamic loading capability. The actuator has a vertical loading capacity of 250 kN and a stroke of ±200 mm, enabling both static and dynamic loading. A force sensor, fabricated from alloy steel and positioned at the actuator's extremity, accurately measures the load applied. Additionally, a bearing plate, sized to match the sample model box, is placed on the sample surface to transmit and distribute the vertical load. Test monitoring data primarily include the vertical displacement of the sample surface. A 2 × 2 array of displacement sensors is utilized, with four corresponding deformation monitoring points located at the bearing plate's corners. The bearing plate's monitored vertical displacement indirectly indicates the sample's overall expansion and compression deformation values. The parameters for the laser displacement sensors are detailed in Table 1.

Table 1. Laser displacement sensors parameters.

Model Number	Measuring Center Distance	Measuring Range	Repeatability	Diameter of Light Speed	Straightness	Supply Voltage	Installation Mode
HG-C1200	200 mm	±80 mm	70 μm	About 50 μm	±0.1% F.S	24 V	Support

2.2. Experiment Method

The sandstone and mudstone samples utilized in the experiment were sourced from the section of a high-speed railway in Guangxi, which is characterized by weak expansive rock subgrades. The samples, extracted on-site, underwent processes of hammering, air-drying, crushing, and sieving before being set aside for use. Their fundamental physical properties were ascertained through laboratory testing, as detailed in Table 2.

This study focuses on the interbedded structure of sandstone and mudstone as the research subject, examining the impact of three factors: the ratio of sandstone to mudstone layer thickness, the occurrence of rock strata, and the applied overlying load. These factors are considered in relation to the expansion and compression deformation characteristics of interbedded weak expansive rocks when immersed in water. To investigate each factor, three distinct design schemes are implemented, resulting in a total of 27 experimental groups. The specific parameters for these experiments are detailed in Table 3.

Table 2. Fundamental physical properties of rock samples for testing.

Rocks Samples	Natural Water Content (%)	Natural Density (g/cm³)	Dry Density (g/cm³)	Particle Density (g/cm³)	Optimal Water Content (%)	Single-Axis Compressive Strength (MPa)		Expansion Ratio (%)	Expansion Force (MPa)	Cohesive Force (MPa)
						Natural	Drying			
Mudstone	19.17	2.07	2.47	2.77	21	0.964	20.4	1.3	0.055	11.3
Sandstone	13.19	2.30	2.60	2.69	13	0.748	6.98	0.1	0.015	30.0

Table 3. Values of experiment parameters.

Level	Investigation Factors		
	Thickness Ratio (Sandstone: Mudstone)	Occurrence	Loading
1	1:1	Flat Layer (the inclination angle is 0°)	0 kPa
2	2:1	Oblique Layer (the inclination angle is 30°)	12.5 kPa
3	3:1	Vertical Layer (the inclination angle is 90°)	25 kPa

According to the geological survey report of the sampling site area, only the rock mass in the range of atmospheric and immersion influence depth was considered, and the thickness ratio of sandstone layer to mudstone layer fluctuates within the range of 0.74:1~4.56:1. In order to facilitate the experimental design and make the test results representative [8,40,41], three levels of 1:1, 2:1 and 3:1 were selected in this study. On this basis, the influence of layer thickness ratio on the expansion and compression deformation of weak expansive rock with interbedded structure was investigated.

Referring to 'TB 10102-2023 Specification for Soil Test of Railway Engineering' [43], sandstone and mudstone samples were individually stirred and wetted at their respective optimal water contents during the experiment. The prepared loose rock samples were then transformed into interbedded structure samples using static pressure method, with the sandstone samples exhibiting a brown color and the mudstone samples a reddish-brown hue. The concrete sample filling scheme is illustrated in Figure 2.

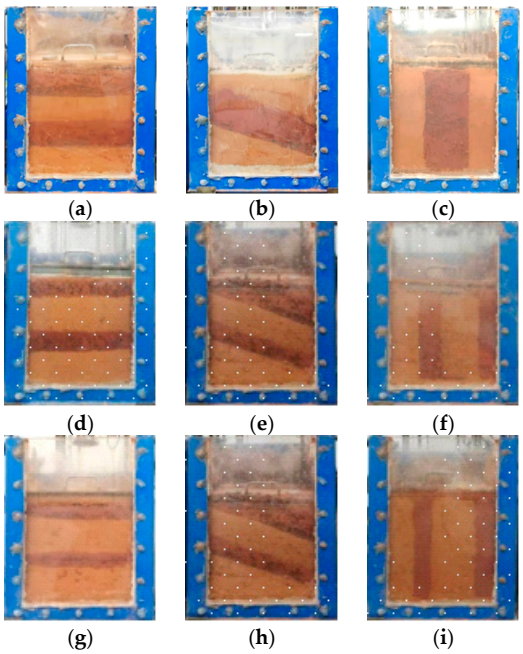

Figure 2. Sample filling scheme diagram: (**a**) Thickness Ratio 1:1–Flat Layer; (**b**) Thickness Ratio 1:1–Oblique Layer; (**c**) Thickness Ratio 1:1–Vertical Layer; (**d**) Thickness Ratio 2:1–Flat Layer; (**e**) Thickness Ratio 2:1–Oblique Layer; (**f**) Thickness Ratio 2:1–Vertical Layer; (**g**) Thickness Ratio 3:1–Flat Layer; (**h**) Thickness Ratio 3:1–Oblique Layer; (**i**) Thickness Ratio 3:1–Vertical Layer.

Once the sample filling is complete, water is gradually introduced into the sample model box through the water valve until the bearing plate's surface is submerged. Throughout the loading process, a thin layer of water consistently covers the surface of the bearing plate. The displacement sensor array is employed to capture the time history data of the bearing plate's vertical displacement changes under the influence of various factors. These data serve as an indicator to indirectly measure the overall expansion and compression deformation of the sample. Once the expansion and compression deformation stabilize, flooding and loading can cease. Subsequently, the sample model box's contents, including the samples and water, are removed. The next cycle of flooding and loading can then commence after the samples have been replenished according to the subsequent filling scheme.

3. Analysis of Experiment Results

3.1. Orthogonal Experimental Analysis

In light of the extensive workload and the considerable time required for comprehensive experiments, an orthogonal experiment was employed in this study to perform a preliminary analysis of the factors that influence the expansion and compression deformation characteristics of interbedded weak expansive rocks when immersed in water. An $L_9(3^4)$ orthogonal array, encompassing four factors at three levels each, was designed to acquire the expansion and compression deformation data of the sample upon reaching stability under the condition of a combination of all factors. Subsequently, a range analysis of the test data was conducted, as presented in Table 4.

Table 4. Orthogonal experiment table.

Test Number	A (Thickness Ratio)	B (Occurrence)	C (Loading)	D (Blank Column)	Expansion and Compression Deformation Value (mm)
1	1	1	1	1	2.28
2	1	2	3	2	−0.61
3	1	3	2	3	−0.22
4	2	1	3	3	−0.06
5	2	2	2	1	−0.19
6	2	3	1	2	1.12
7	3	1	2	2	0.10
8	3	2	1	3	0.99
9	3	3	3	1	−0.20
K_1	1.450	2.320	4.390	1.890	
K_2	0.870	0.190	−0.310	0.610	
K_3	0.890	0.700	−0.870	0.710	
k_1	0.483	0.773	1.463	0.630	
k_2	0.290	0.063	−0.103	0.203	
k_3	0.297	0.233	−0.290	0.237	
R	0.193	0.710	1.753	0.427	

The effect curve, as depicted in Figure 3, is derived from the data presented in Table 4.

Figure 3 clearly illustrates that the loading is the predominant factor influencing the expansion and compression deformation of sandstone intercalated with mudstone. This is followed by the occurrence and the thickness ratio. As these factors increase, the samples tend to undergo compression deformation. It is evident that as the ratio of sandstone to mudstone layer thickness increases, the mudstone content diminishes progressively. Consequently, the interior content of the hydrophilic clay minerals also decreases, which is manifested in the reduced expansion deformation of the water-saturated sample. The overlying load significantly inhibits the water-immersed expansion deformation of weak expansive rocks. Thus, with an increase in the loading, the expansion deformation of the weak expansive rocks with an interbedded structure also gradually diminishes. When the loading value escalates to match the expansive force of the sample, the expansion defor-

mation reaches zero; if the loading continues to rise, the sample undergoes compressive deformation. Among these nine sets of experiments, the minimum value for deformation is −0.61 mm (indicating compression deformation), while the maximum value is 2.28 mm (indicating expansion deformation), with a minimum absolute value of −0.06 mm. The factor combinations corresponding to these three groups are A1B2C3, A1B1C1, and A2B1C3, respectively. Based solely on the result data, it is challenging to precisely determine the impact of rock occurrence on the water-immersed expansion and compression deformation of sandstone intercalated mudstone samples. However, it can be tentatively deduced that an increase in the rock inclination angle restricts the expansion deformation of weak expansive rocks, a hypothesis that requires further validation through subsequent experiments.

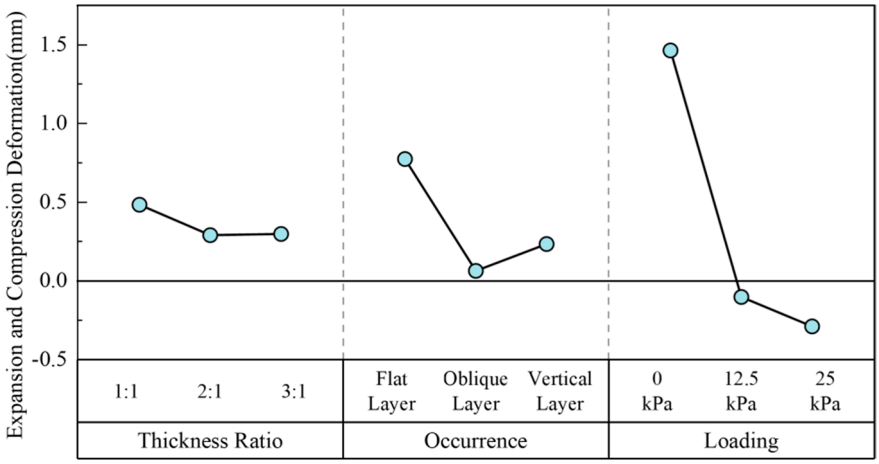

Figure 3. Orthogonal experiment effect curve.

3.2. Expansion and Compression Deformation Trend Analysis

To elucidate the impact of diverse factors on the expansion and compression deformation behaviors of sandstone intercalated with mudstone interbedded structure samples, three parameters—thickness ratio, occurrence, and loading—were designated as control variables. The stable expansion and compression deformation of the samples under uniform control conditions were portrayed through a 3D mapping surface, generated by the integration of these factors. This approach allowed for a visual representation of the sample's expansion and compression deformation characteristics. The ensuing analysis outcomes are delineated in the subsequent sections.

3.2.1. Thickness Ratio as Control Condition

The 3D mapping surfaces in Figure 4 illustrate the stable expansion and compression deformation of samples under combinations of factors at various thickness ratios. From this figure, it is evident that for different layer thickness ratios, the stability value of the water-immersed expansion and compression deformation of weak expansive rocks with sandstone intercalated with mudstone shows a consistent trend with changes in occurrence and loading level. This trend is characterized by significant expansion deformation when the flat layer is unloaded and substantial compression deformation when the vertical layer is subjected to 25 kPa. As the rock inclination angle increases gradually along with the loading grade, the expansion deformation of the sample decreases progressively, transitioning from expansion to compression deformation.

Overall, as the layer thickness ratio continues to rise, the absolute value of the sample's expansion and compression deformation also diminishes gradually, which is represented by a lighter color on the 3D mapping surface. Analysis indicates that an increased layer thickness ratio leads to a reduction in mudstone content within the sample. This limits the expansion deformation caused by the water absorption of hydrophilic mineral components, allowing the accumulated expansion deformation to easily dissipate along the sandstone layer. During compression deformation, the decreased mudstone content also results in

fewer internal pores. Consequently, the dynamic expansion of mudstone rapidly fills these pores, hindering particle sliding and compaction. Moreover, since the sandstone is relatively dense, the overall compressible space within the sample of expansible rock with a weak interbedded structure is limited, resulting in a smaller absolute value of compression deformation.

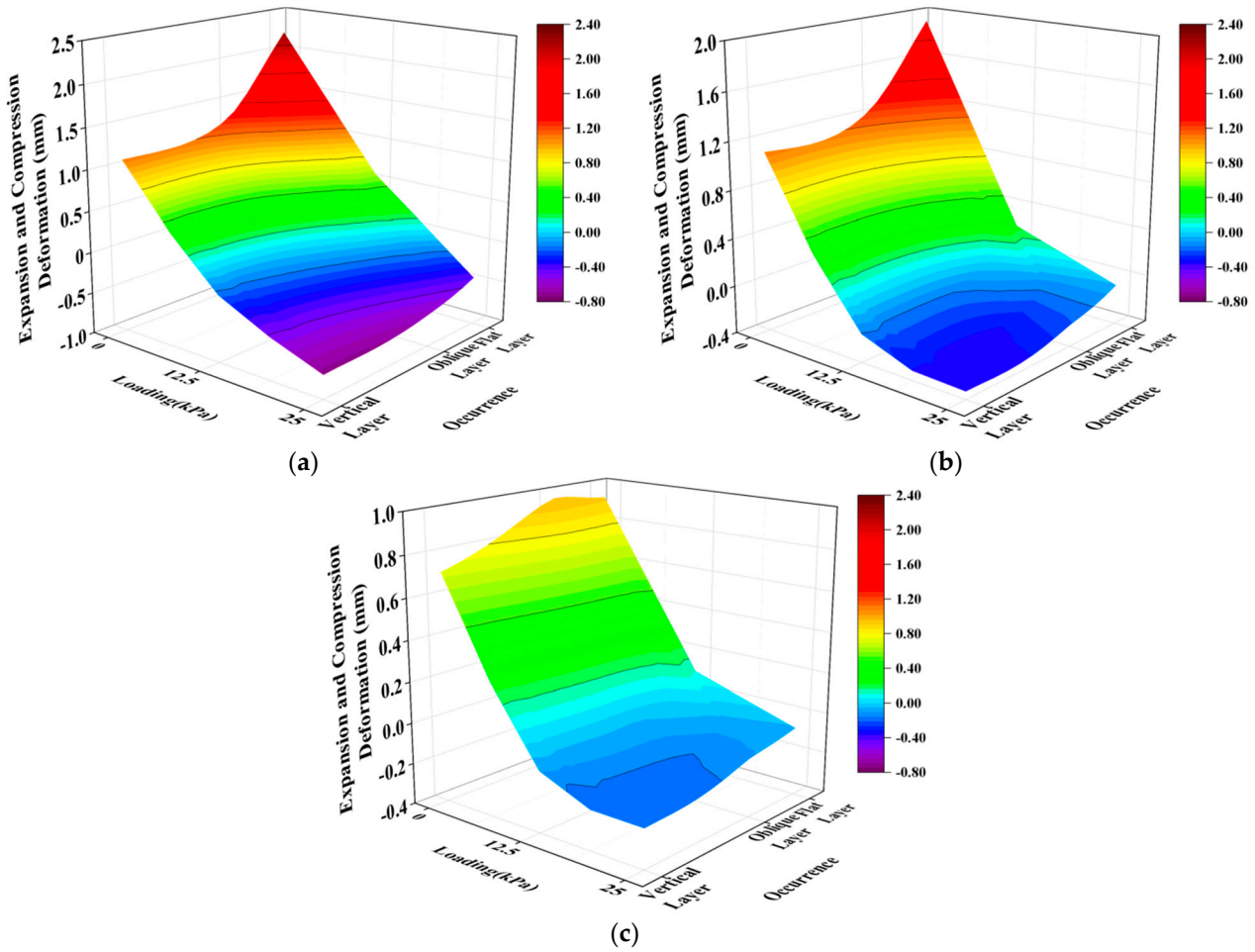

Figure 4. Three-dimensional mapping surfaces at different thickness ratio levels: (**a**) Thickness Ratio 1:1; (**b**) Thickness Ratio 2:1; (**c**) Thickness Ratio 3:1.

3.2.2. Occurrence as Control Condition

The 3D mapping surfaces illustrating the stable expansion and compression deformation of samples, as influenced by the combinations of various factors at different occurrence levels, are depicted in Figure 5.

Figure 5 illustrates that the alteration in rock occurrence does not influence the pattern of expansion and compression deformation characteristics for weak expansive rocks with a sandstone intercalated mudstone interbedded structure when immersed in water. In the expansive deformation segment, an increase in the layer thickness ratio results in a decrease in the value of expansion deformation. Conversely, in the compressive deformation segment, the absolute value of compression deformation for weak expansive rock samples with an interbedded structure diminishes progressively as the thickness ratio increases. The impact of the loading on sample expansion and compression deformation remains predominant, with peak values of expansion and compression deformation occurring at thickness ratios of 1:1 under 0 kPa and 1:1 under 25 kPa, respectively. The cause analysis aligns with previous discussions.

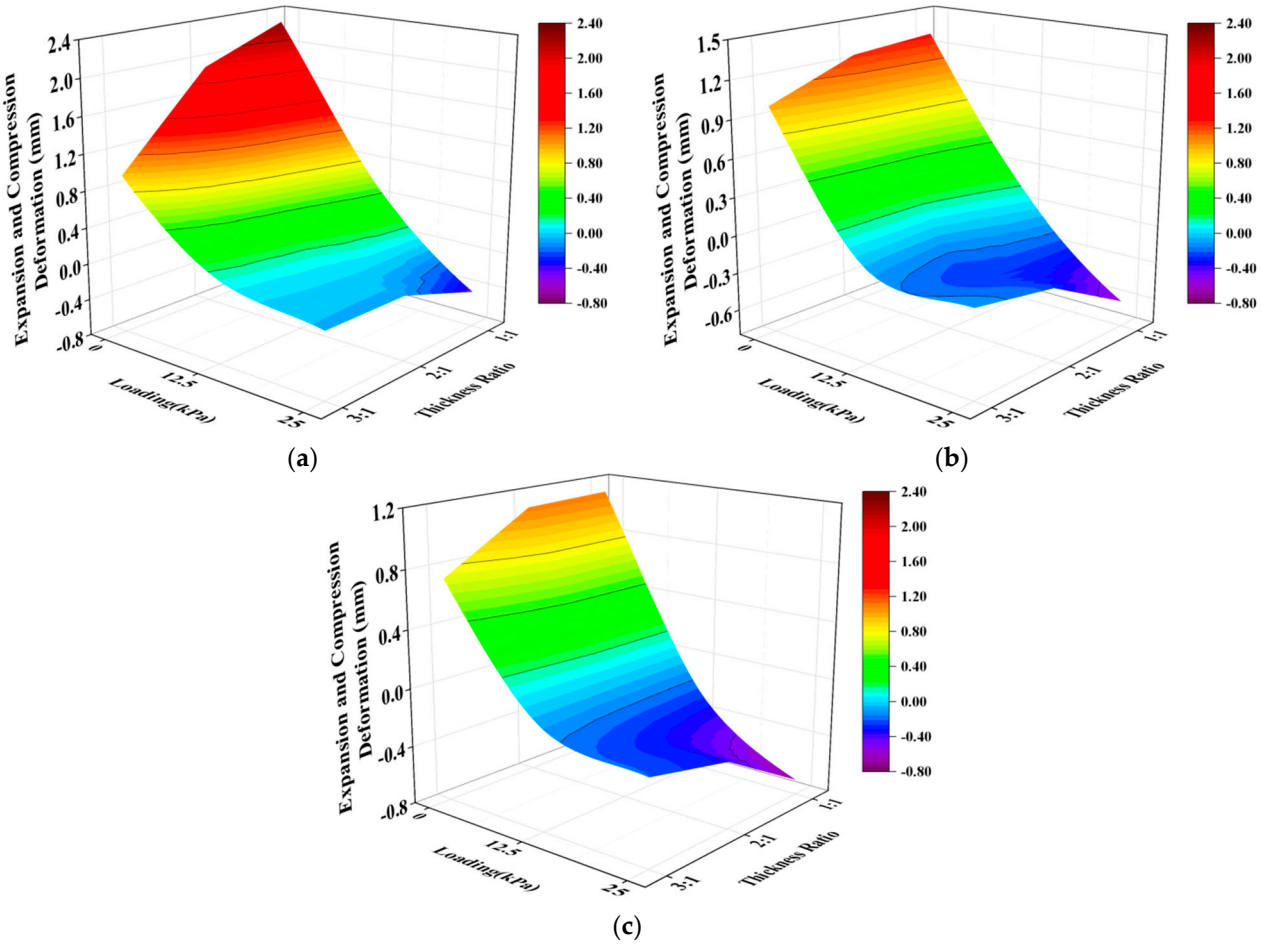

Figure 5. Three-dimensional mapping surfaces at different occurrence levels: (**a**) Flat Layer (0°); (**b**) Oblique Layer (30°); (**c**) Vertical Layer (90°).

As the inclination angle of the sandstone and mudstone interbedded structure sample increases, the overall expansion deformation of the sample progressively diminishes, while the compression deformation augments. In other words, the sample's overall deformation evolves from expansion to compression, particularly evident when the layer thickness ratio is 1:1–25 kPa. Analysis indicates that the experiment primarily gauges the surface expansion and compression deformation of the sample, constrained by lateral deformation as a whole. Given a constant layer thickness ratio—that is, constant mudstone content—the vertical deformation of the sample is dictated by the horizontal area of the sample, which correlates with the rock layer's inclination angle. A greater inclination angle results in a reduced effective expansion area for the weak expansive rock in the horizontal direction. Consequently, the cumulative amount of mudstone's expansion deformation decreases, and with the same mudstone content, the entire sample exhibits equivalent potential for compression deformation. The dynamic equilibrium between expansion and compression deformation within the microscopic mudstone sample continues to favor compression deformation, leading to the transformation from expansion to compression deformation after the sample is fully submerged in water and stabilized. Whether this deformation trend can be quantitatively computed using theoretical formulas requires further investigation.

3.2.3. Loading as Control Condition

The 3D mapping surfaces in Figure 6 illustrate the stable expansion and compression deformation of the samples under various loading levels and combinations of different factors. From Figure 6, it is evident that when the loading is considered as a control condition, it becomes challenging to uniformly describe the deformation behavior of samples in

conditions of water immersion, expansion, and compression. Nevertheless, on an overall basis, there is a consistent trend observed: as the loading level increases, irrespective of the layer thickness ratio or the level of rock occurrence, the weak expansive rock samples of sandstone intercalated with mudstone tend to shift from exhibiting expansion deformation to exhibiting compression deformation. The loading stands out as the most influential factor affecting the expansion and compression deformation of the sample.

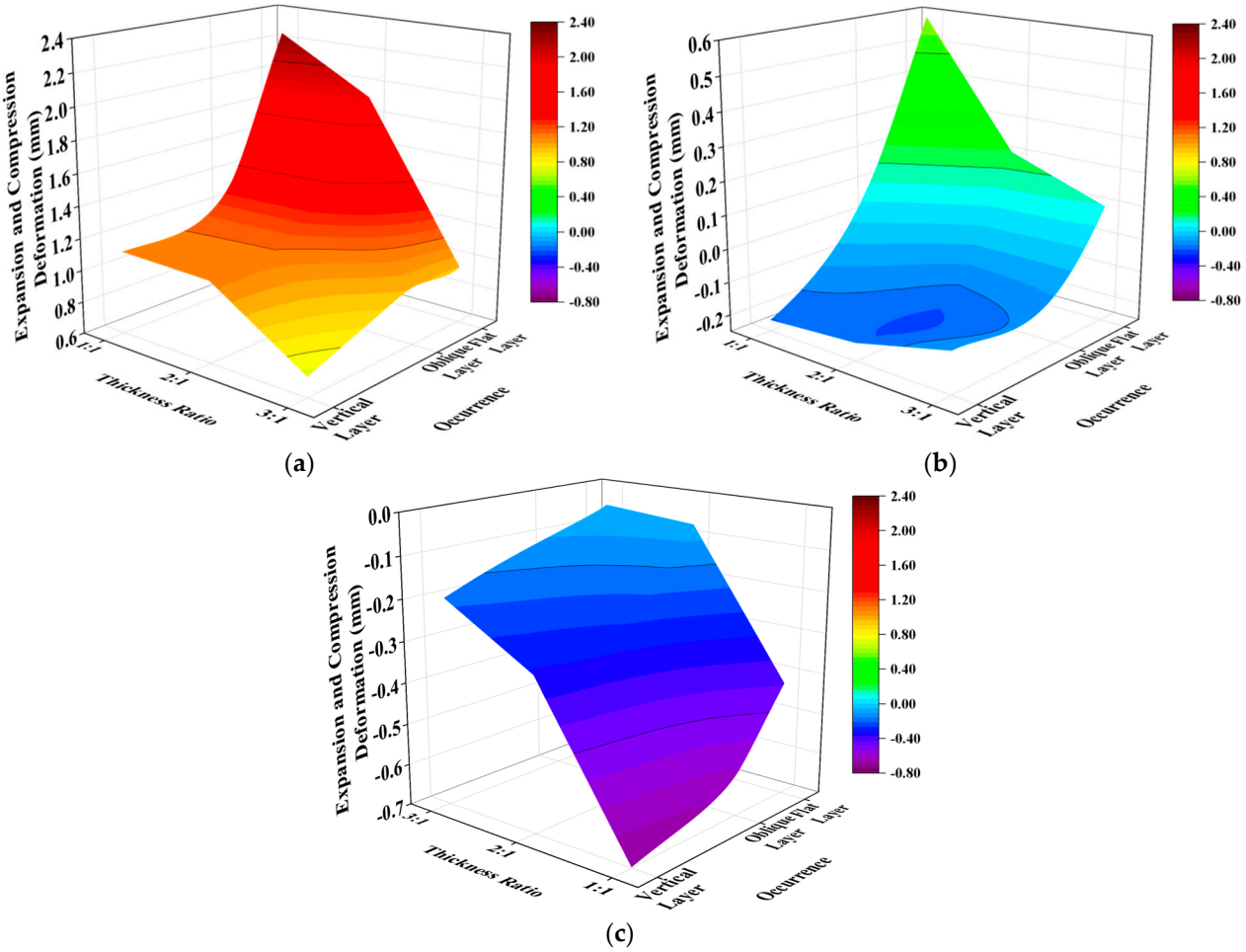

Figure 6. Three-dimensional mapping surfaces at different loading levels: (**a**) 0 kPa; (**b**) 12.5 kPa; (**c**) 25 kPa.

Under 0 kPa conditions, as depicted in Figure 6a, the sample undergoes expansion deformation for all combinations of a variety of factors. The maximum and minimum expansions are observed at 2.28 mm and 0.72 mm, respectively, notably evident when the layer thickness ratio is either 1:1 (flat layer) or 3:1 (vertical layer). It is apparent that the expansion deformation diminishes with an increase in both the layer thickness ratio and the rock inclination angle.

When subjected to a loading of 12.5 kPa, as illustrated in Figure 6b, the sample consistently demonstrates expansion deformation in flat layer structures and compression deformation in vertical layer structures, irrespective of the layer thickness ratio. This behavior signifies that the overall expansive force within the sample diminishes progressively with an increment in the rock inclination angle. When the rock layer's inclination ranges between 0° and 90°, the total expansive force of the sample precisely counterbalances the overburden load of 12.5 kPa.

As the loading increases to 25 kPa, as depicted in Figure 6c, the entire sample exhibits compression deformation. In this instance, the impact of the layer thickness ratio on the

sample's expansion and compression behavior in water immersion significantly outweighs the occurrence of rock strata. Furthermore, when the layer thickness ratio is at least 2:1, the overall expansion and compression behavior of the sample remains largely unaltered. If the foundation contains a relatively small amount of weak expansive rocks, it is unnecessary to consider the influence of rock occurrence. Instead, it suffices to manage the overlying load value of the weak expansive rocks through embankment filling reinforcement design, ensuring that expansion deformation does not occur. This approach minimizes the need for extensive land replacement, thereby reducing the overall cost of the project.

3.3. Time-History Analysis of Expansion and Compression Deformation

The prior discussion primarily concentrates on the stability value associated with the deformation of a sandstone intercalated with mudstone interbedded structure under conditions of water immersion. However, in practical engineering applications, it is imprudent to concentrate solely on this particular value. The rate of deformation is an additional parameter that necessitates monitoring.

Considering the scarcity of engineering cases involving vertical layer (90° inclination angle) weak expansive rock formations with interbedded structures, this study focuses on analyzing test results for flat layer (0° inclination angle) and oblique layer (30° inclination angle). The time-history curves depicting the expansion and compression deformation of both the flat and oblique layer samples were plotted. These curves were subsequently fitted with hyperbolic functions, with the specific results being displayed in Figure 7.

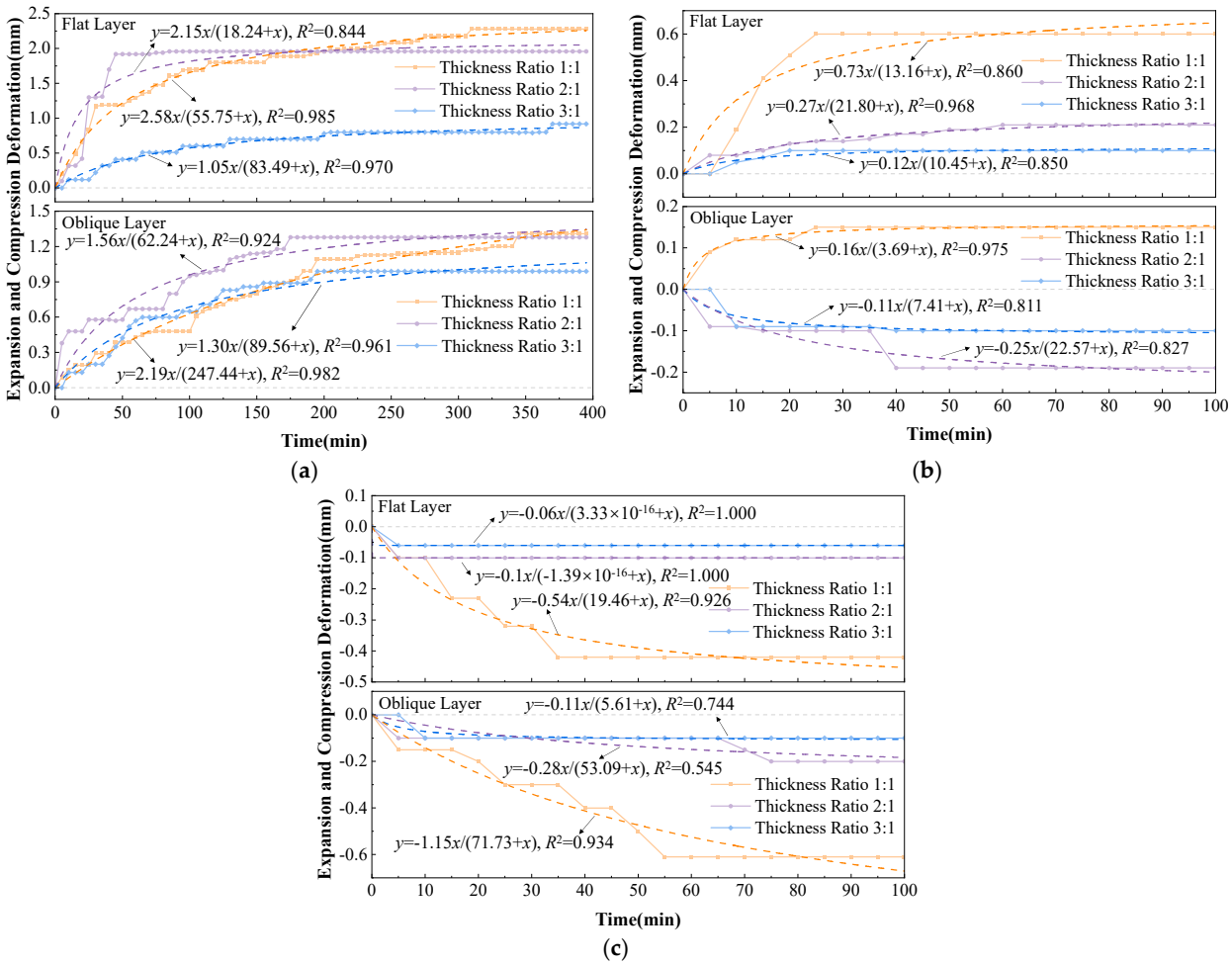

Figure 7. The time–history curves of samples' expansion and compression deformation: (**a**) 0 kPa; (**b**) 12.5 kPa; (**c**) 25 kPa.

As depicted in Figure 7, for the flat layer structure, the samples' expansion forces of different layer thickness ratios oscillate between 12.5 and 25 kPa. Regarding the oblique layer structure, when the layer thickness ratio is 1:1, the expansion force ranges from 12.5 to 25 kPa; however, when the ratio exceeds 1:1, the expansion force diminishes to a span of 0 to 12.5 kPa. Moreover, the rate at which the sample's expansion and compression deformation stabilizes under a load is substantially faster compared to its unloaded state. Specifically, in the absence of a load, the sample requires at least 5~7 h to achieve a stable deformation state, whereas under a load, this stabilization occurs within approximately 1 h. Additionally, when the applied load approaches or surpasses the sample's expansion force, deformation can rapidly progress. There appears to be no substantial disparity in the duration of the stability period. It can thus be inferred that in the context of a subgrade construction within regions characterized by weak expansive rocks with an interbedded structure, the compactness of the site can potentially be enhanced through precompression, tamping, and other such techniques. Consequently, maintaining a relatively high level of overlying load on the interbedded structure could significantly abbreviate the time required for the foundation to reach a stable deformation state post-construction.

The time-history curves of expansion and compression deformation that demonstrated a superior hyperbolic fitting effect were selected. Subsequently, the first-order derivatives of these fitting curves were calculated, respectively. This enabled the plotting of the sample's deformation rate over time under the influence of various factors, as depicted in Figure 8.

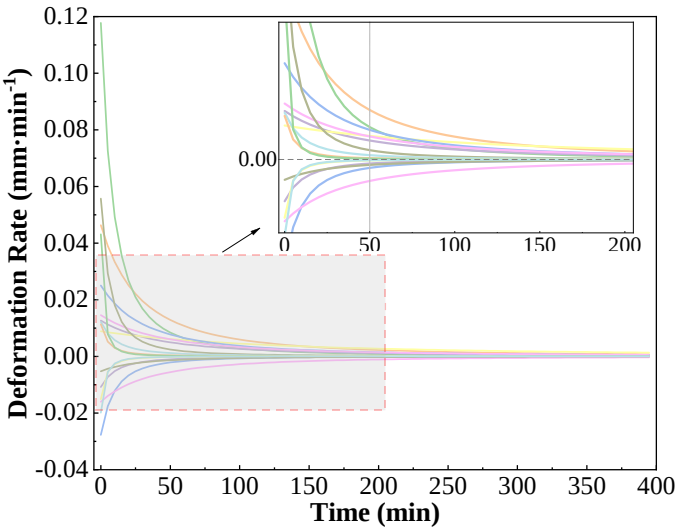

Figure 8. Deformation rate—time relation curves.

An analysis of Figure 8 reveals that irrespective of whether the sample is undergoing expansion or compression deformation, the deformation rate remains relatively high between 0 and 50 min after immersion. During this period, the deformation progresses rapidly, yet the rate of deformation diminishes quickly. From 50 to 200 min, the samples' expansion and compression deformation rates enter a phase of gradual decline, ultimately approaching zero, indicating a slow progression toward a stable state. Post 200 min, the rates of expansion and compression deformation are significantly reduced, suggesting that the samples have achieved a stable condition in terms of their deformation development.

The expansion and compression deformation process of a weak expansive rock sample with sandstone intercalated with mudstone interbedded structure can be categorized into three distinct stages: rapid deformation, slow deformation, and completed development. In the rapid deformation stage, the samples' expansion and compression deformation develops rapidly, potentially reaching 90% of the final stable state under loading. In the subsequent slow deformation stage, the rate of deformation development decreases, nearing completion, with minimal incremental changes in the expansion and compression values. Finally, in the completed development stage, any further expansion and compres-

sion deformation is virtually halted, rendering its impact on the superstructure in practical engineering applications negligible.

3.4. Expansion Force Fitting

The analysis presented above indicates that the expansion and compression deformation characteristics of weak expansive rocks with an interbedded structure, when immersed in water, are most significantly influenced by the overlying load. The expansion and compression deformation of such rock can be effectively managed by regulating the value of the overlying load. Consequently, determining the expansion force of weak expansive rock with an interbedded structure is crucial for constructing a high-speed railway subgrade in areas characterized by this type of rock.

Previous research indicates that the expansion deformation of expansive rock (or soil) exhibits an inverse correlation with the overlying load. The vertical axis represents the expansion and compression deformation of the sample, while the horizontal axis denotes the corresponding load values. A relationship curve between the expansion and compression deformation and the overlying load is plotted, which is subject to nonlinear fitting. The x-coordinate value at the intersection of the fitted curve with y = 0 represents the expansion force of the sample under the current factor level. The fitting curve for the sample, considering the combined effect of various factors on the expansion and compression deformation versus the loading, is illustrated in Figure 9.

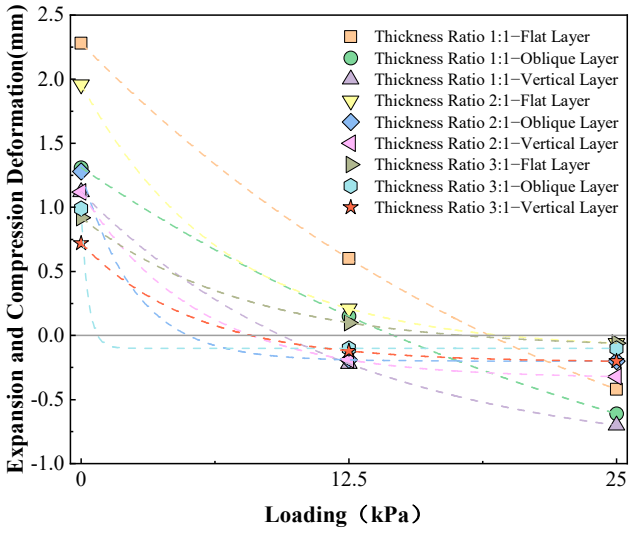

Figure 9. Expansion and compression deformation—Loading fitting curve.

The x-coordinate values of each fitted curve at the intersection with y = 0 are presented as follows.

The data presented in Table 5 are graphically represented on a 3D mapping surface, as depicted in Figure 10.

From Figure 10, it is evident that the expansion force of the weak expansive rock sample, characterized by an interbedded structure of sandstone and mudstone, diminishes as the layer thickness ratio and rock inclination angle increase. The calculated reductions are within the ranges of 8.91% to 38.68% and 51.00% to 58.83%, respectively. The data indicate that the expansion force is more significantly influenced by the rock occurrence level than by the layer thickness ratio.

For projects involving underlying foundations with thin, steeply inclined weak expansive rock layers, the overlying load can be determined through geological surveys and laboratory testing. If the expansion force is within acceptable limits, no additional treatment measures are necessary. In cases where the weak expansive rock layer is shallow, thick, and gently inclined, the expansion force value should be calculated based on the specific project requirements. The embankment surface load level can be maintained by either designing

an appropriate embankment fill height or by excavating the weak expansive rock layer to a certain depth for partial filling. Post-construction, the expansion and compression deformation of the weak expansive rock with the underlying interbedded structure remains at a low level, allowing for rapid and stable development.

Table 5. The expansion force of the sample of each factor level combination.

Thickness Ratio	Occurrence	Expansion Force (kPa)
Thickness Ratio 1:1	Flat Layer	19.08
	Oblique Layer	14.53
	Vertical Layer	9.35
Thickness Ratio 2:1	Flat Layer	19.36
	Oblique Layer	9.09 *
	Vertical Layer	7.97
Thickness Ratio 3:1	Flat Layer	17.38
	Oblique Layer	8.91 *
	Vertical Layer	7.88

* The data were modified by manual fitting.

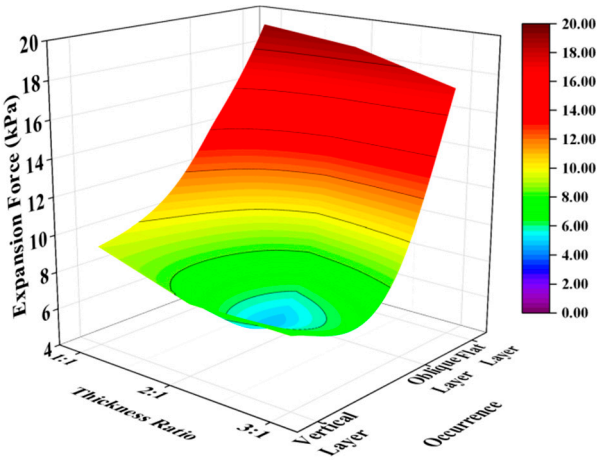

Figure 10. Three-dimensional mapping surface of sample expansion force.

4. Conclusions

Two typical weak expansive rocks, sandstone and mudstone, were selected in this study. Nine sets of weak expansive rock samples with different forms of interbedded structures were prepared, using the layer thickness ratios (1:1, 2:1, and 3:1) and the rock occurrence (flat, oblique, and vertical) as the controlling factors. Then, a total of 27 sets of indoor immersion deformation characteristic tests were designed based on different overburden loadings (0 kPa, 12.5 kPa, 25 kPa). The influence laws of three influencing factors on the expansion and compression deformation of weak expansive rocks with interbedded structures were comprehensively analyzed. The main conclusions are as follows:

1. The overburden loading has the most significant effect on the expansion and compression deformation of sandstone–mudstone interbedded structure samples. Its orthogonal test effect curve showed a clear monotonic decreasing trend and the decrease was the largest. The increase in overburden loading and rock inclination angle will cause the sample to change from expansion to compression deformation. The change in layer thickness ratio will only affect the absolute value of deformation, but will not change the deformation trend of the sample.
2. The expansion and compression deformation of sandstone interbedded with mudstone samples has obvious three-stage characteristics, 0~50 min for the rapid deformation stage, 50~200 min for the slow deformation stage, and 200 min later for the completed development stage. In addition, the deformation stability rate of the sample

under load is obviously faster, which is about 5~7 times that under no load. However, when the overburden loading value exceeds the expansion force of the sample, the difference in the deformation stability period of the sample is not significant.

3. The expansion force of the sample decreases with the increase in the layer thickness ratio level and the inclination angle of the rock layer, and the reduction ranges are 8.91~38.68% and 51.00~58.83%, respectively. Therefore, the influence of rock occurrence on the expansion force of the sample is more significant.

Author Contributions: Conceptualization, Y.W. and Y.L.; methodology, H.Q. and Q.Q.; formal analysis, Y.L., Y.Z., Y.Y., J.J. and T.Z.; investigation, H.Q.; data curation, Y.W., Y.Z. and D.C.; writing—original draft preparation, Y.L. and D.C.; writing—review and editing, Y.W., Y.Y. and J.J.; visualization, Y.L., T.Z. and Q.Q.; supervision, Y.W. and D.C.; project administration, Y.W., Y.Z., Y.Y. and D.C. All authors have read and agreed to the published version of the manuscript.

Funding: This research was sponsored by the Research Fund of the National Natural Science Foundation of China (Grant No. 51808462), the Applied Basic Research Project of Sichuan Science and Technology Department (general project) (Grant No. 2023NSFSC0346), the Inner Mongolia Autonomous Region science and technology planning project (2021GG0038), the Major science and technology project of Hohhot (2021-Key-Social-3), the Science and Technology project of Inner Mongolia Transportation Department (NJ-2022-14), the interdisciplinary research project of the Southwest Jiaotong University (A0920502052301-404), the new interdisciplinary cultivation fund of the Southwest Jiaotong University (YH1500112432284), the China Postdoctoral Science Foundation (Grant No. 2018 M643520), the Applied Basic Research Project of Sichuan Science and Technology Department (Free Exploration Type) (Grant No. 2020YJ0039), and the Key R & D Support Plan of Chengdu Science and Technology Project—Technology Innovation R & D Project (Grant No. 2019-YF05-00002-SN).

Data Availability Statement: The raw data supporting the conclusions of this article will be made available by the authors on request.

Conflicts of Interest: Authors Yaning Wang, Yangui Zhu, Yibo Yao, Jin Jin and Tao Zheng were employed by the company China Railway First Survey and Design Institute Group Co., Ltd. The remaining authors declare that the research was conducted in the absence of any commercial or financial relationships that could be construed as a potential conflict of interest.

References

1. Liu, X.; Chen, X.; Song, X. Physical simulation test on deformation and failure mechanism of soft and hard interbedded rock masses. *Chin. J. Rock Mech. Eng.* **2023**, *42*, 3980–3995. [CrossRef]
2. Liu, Z.; Zhang, R.; Lan, T.; Zhou, Y.; Huang, C. Laboratory test and constitutive model for quantifying the anisotropic swelling behavior of expansive soils. *Appl. Sci.* **2024**, *14*, 2255. [CrossRef]
3. Li, H.; Wang, J.; Li, H.; Wei, S.; Li, X. Experimental study on deformation and strength characteristics of interbedded sandstone with different interlayer thickness under uniaxial and triaxial compression. *Processes* **2022**, *10*, 285. [CrossRef]
4. Wang, R.; Cheng, J.; Gao, L.; Li, Z.; Qi, Y.; Wang, M.; Ding, B. Research on the swelling mechanism of high-speed railway subgrade and the induced railway heave of ballastless tracks. *Transp. Geotech.* **2021**, *27*, 100470. [CrossRef]
5. Maheshwari, P. Analysis of deformation of linear viscoelastic two layered laminated rocks. *Int. J. Rock Mech. Min. Sci.* **2021**, *141*, 104681. [CrossRef]
6. Wu, Q.; Liu, Y.; Tang, H.; Kang, J.; Wang, L.; Li, C.; Wang, D.; Liu, Z. Experimental study of the influence of wetting and drying cycles on the strength of intact rock samples from a red stratum in the Three Gorges Reservoir area. *Eng. Geol.* **2023**, *314*, 107013. [CrossRef]
7. Tian, Y.; Wu, F.; He, L.; Tian, H.; Huang, M.; Chen, W. Investigation of 3D printing sand core technology on the mechanical behaviors of soft–hard interbedded rock masses. *J. Mater. Civ. Eng.* **2023**, *35*, 04023440. [CrossRef]
8. Luo, P.; Li, D.; Ma, J.; Zhou, A.; Zhang, C. Experimental investigation on mechanical properties and deformation mechanism of soft-hard interbedded rock-like material based on digital image correlation. *J. Mater. Res. Technol.* **2023**, *24*, 1922–1938. [CrossRef]
9. Qin, Y.; Yang, G.; Liu, B.; Xu, J. Study on deformation and failure mechanism of low-dip red bed slope with soft-hard interbedded structure: A case study of Chishui, China. *Nat. Hazards* **2024**, 1–19. [CrossRef]
10. Chen, G.; Cai, P.; Zhan, J.; Yang, Y.; Yao, Z.; Yu, Z. Deformation patterns and failure mechanisms of soft-hard-interbedded anti-inclined layered rock slope in Wolong open-pit coal mine. *Appl. Sci.* **2024**, *14*, 3082. [CrossRef]
11. Dai, Z.; Huang, K.; Chi, Z.; Chen, S. Model test study on the deformation and stability of rainfall-induced expansive soil slope with weak interlayer. *Bull. Eng. Geol. Environ.* **2024**, *83*, 76. [CrossRef]

12. Goodman, R.; Bray, J. Toppling of rock slopes. proceedings, specialty conference on rock engineering for foundations and slopes. *Boulder* **1976**, *2*, 739–760.
13. Zhang, B.; Tang, H.; Fang, K.; Ding, B.; Gong, Q. Experimental study on deformation and failure characteristics of interbedded anti-inclined rock slopes induced by rainfall. *Rock Mech. Rock Eng.* **2024**, *57*, 2933–2960. [CrossRef]
14. Zhang, B.; Tang, H.; Sumi, S.; Ding, B.; Zhang, L.; Ning, Y. Exploring the deformation and failure characteristics of interbedded anti-inclined rock slopes: Insights from physical modelling tests. *Rock Mech. Rock Eng.* **2024**, *57*, 1603–1628. [CrossRef]
15. Dong, M.; Zhang, F.; Lv, J.; Hu, M.; Li, Z. Study on deformation and failure law of soft-hard rock interbedding toppling slope base on similar test. *Bull. Eng. Geol. Environ.* **2020**, *79*, 4625–4637. [CrossRef]
16. Ye, W.; Gao, C.; Liu, Z.; Wang, Q.; Su, W. A Fuzzy-AHP-based variable weight safety evaluation model for expansive soil slope. *Nat. Hazards* **2023**, *119*, 559–581. [CrossRef]
17. Wyllie, D.; Wood, D. Stabilization of toppling rock slope failures. In Proceedings of the 33rd Highway Geology Symposium, Engineering Geology and Environmental Constraints in Vail, Colorado, 1982; Colorado Geological Survey: Denver, CO, USA, 1983.
18. Wyllie, D. Toppling rock slope failures-examples of analysis and stabilization. *Rock Mech.* **1980**, *13*, 89–98. [CrossRef]
19. Liu, Y.; Huang, D.; Peng, J.; Guo, Y. Analysis of the effect of rock layer structure on the toppling failure evolution of soft-hard interbedded anti-dip slopes. *Eng. Fail. Anal.* **2023**, *145*, 107005. [CrossRef]
20. Wang, R.; Zheng, Y.; Chen, C.; Zhang, W. Theoretical and numerical analysis of flexural toppling failure in soft-hard interbedded anti-dip rock slopes. *Eng. Geol.* **2023**, *312*, 106923. [CrossRef]
21. Yu, J. Study on reasonable construction method for tunnels in contact zone of red clay and sandstone interbedded with mudstone. *Mod. Tunn. Technol.* **2021**, *58*, 174–181. [CrossRef]
22. Zhao, D.; Ji, Q.; Wang, G. Research on mechanical characteristics of large-span tunnels in bedding mudstone with sandstone strata. *Tunn. Constr.* **2021**, *41*, 740–748. [CrossRef]
23. Zhao, D.; He, Q.; Ji, Q.; Wang, F.; Tu, H.; Shen, Z. Similar model test of a mudstone-interbedded–sandstone-bedding rock tunnel. *Tunn. Undergr. Space Technol.* **2023**, *140*, 105299. [CrossRef]
24. Liu, W.; Chen, J.; Chen, L.; Luo, Y.; Shi, Z.; Wu, Y. Deformation evolution and failure mechanism of monoclinic and soft-hard interbedded strata: Study of muzhailing tunnel. *J. Perform. Constr. Facil.* **2021**, *35*, 04021042. [CrossRef]
25. Chen, J.; Liu, W.; Chen, L.; Luo, Y.; Li, Y.; Gao, H.; Zhong, D. Failure mechanisms and modes of tunnels in monoclinic and soft-hard interbedded rocks: A case study. *KSCE J. Civ. Eng.* **2020**, *24*, 1357–1373. [CrossRef]
26. Zhang, Z.; Wang, T. Failure modes of weak interlayers with different dip angles in red mudstone strata, Northwest China. *Bull. Eng. Geol. Environ.* **2023**, *82*, 156. [CrossRef]
27. Wang, T.; Yan, C. Investigating the influence of water on swelling deformation and mechanical behavior of mudstone considering water softening effect. *Eng. Geol.* **2023**, *318*, 107102. [CrossRef]
28. Dai, Z.; Guo, J.; Yu, F.; Zhou, Z.; Li, J.; Chen, S. Long-term uplift of high-speed railway subgrade caused by swelling effect of red-bed mudstone: Case study in Southwest China. *Bull. Eng. Geol. Environ.* **2021**, *80*, 4855–4869. [CrossRef]
29. Wang, B.; Wang, Q.; Zhang, R.; Wang, T.; Zhang, T.; Liang, K. Large scale model test of water swelling deformation of mudstone under lateral confinement. *J. Disaster Prev. Mitig. Eng.* **2020**, *40*, 337–342. [CrossRef]
30. Xue, Y.; Wang, Q.; Ma, L.; Wang, B.; Zhang, T. Experimental study on in-situ flooding response characteristics of mudstone foundation for high-speed railway. *J. China Railw. Soc.* **2020**, *42*, 144–150. [CrossRef]
31. Yang, G.; Ding, J. Model test on expansion and shrinkage deformation in expansive soil roadbed. *China J. Highw. Transp.* **2006**, *19*, 23–29. [CrossRef]
32. Duan, J.; Yang, G.; Liu, Y.; Kan, J.; Qiu, M. Deformation characteristics of double-line ballastless track subgrade under water immersion of expansive rock foundation. *J. Cent. South Univ. Sci. Technol.* **2020**, *51*, 156–164. [CrossRef]
33. Cui, X.; Wang, Q.; Zhang, R.; Wang, C.; Xue, Y. Expansive deformation test on ballastless track of expansive mudstone. *J. Railw. Sci. Eng.* **2017**, *14*, 2339–2344. [CrossRef]
34. Cao, Z. Field soaking tests on the moderate-strong expansive soil ground of the high-speed railway subgrade. *J. Railw. Sci. Eng.* **2022**, *19*, 3467–3476. [CrossRef]
35. Duan, J.; Yang, G.; Liu, Y.; Kan, J.; Zhang, L. Influence of water immersion on mechanical and deformation behaviors of expansive soil subgrade for ballastless track. *J. China Railw. Soc.* **2022**, *44*, 119–126. [CrossRef]
36. Zhao, S.; Zheng, J.; Yang, J. Stability analysis of embankment slope considering water absorption and softening of subgrade expansive soil. *Water* **2022**, *14*, 3528. [CrossRef]
37. Lan, T.; Zhang, R.; Yang, B.; Meng, X. Influence of swelling on shear strength of expansive soil and slope stability. *Front. Earth Sci.* **2022**, *10*, 849046. [CrossRef]
38. Li, J.; Wang, Q.; Zhang, R.; Zhang, T.; Wang, T.; Liang, K. Experimental study on swelling law of expansive soil during humidification. *Hydro-Sci. Eng.* **2018**, *3*, 86–94. [CrossRef]
39. Zuo, Q.; Li, P.; Li, X.; Chen, F. Swelling damage evolution of argillaceous slate in a water-rich environment. *Q. J. Eng. Geol. Hydrogeol.* **2023**, *56*, qjegh2022-128. [CrossRef]
40. Kang, Y.; Gu, J.; Wei, M. Mechanical properties and acoustic emission characteristics of soft-hard interbedded rocks under different loading rates. *J. Northeast. Univ. (Nat. Sci.)* **2023**, *44*, 399–407. [CrossRef]
41. Huang, F.; Zhou, Y.; Li, T.; Hu, X. Laboratory experimental study on mechanical properties and failure modes of soft and hard interbedded rock mass. *J. China Coal Soc.* **2020**, *45*, 230–238. [CrossRef]

42. Han, B.; Fu, Q.; Wang, C. Numerical simulation for creep characteristics of soft and hard interphase rock mass. *J. Phys. Conf. Ser.* **2020**, *1600*, 012075. [CrossRef]
43. *TB 10102-2023*; Specification for Soil Test of Railway Engineering. China Railway Publishing House: Beijing, China, 2023.